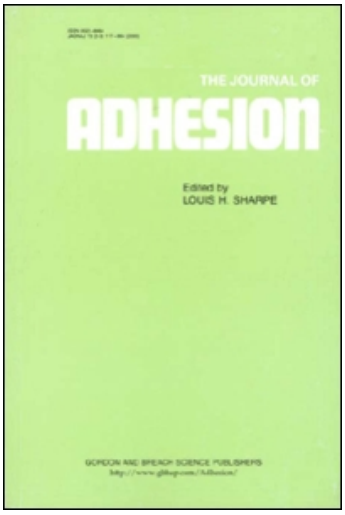

The Journal of Adhesion
Publication details, including instructions for authors and subscription information:
http://www.informaworld.com/smpp/title~content=t713453635

A Model for the Diffusion of Moisture in Adhesive Joints. Part III: Numerical Simulations

S. Roy[a]; D. R. Lefebvre[b]; D. A. Dillard[c]; J. N. Reddy[c]
[a] Engg. Sci. & Mechanics Dept., Blacksburg, VA, U.S.A. [b] Matls. Engg. Science Dept., Virginia Tech., Blacksburg, VA, U.S.A. [c] Engg. Sci. & Mechanics Dept., Virginia Tech., Blacksburg, VA, U.S.A.

To cite this Article Roy, S. , Lefebvre, D. R. , Dillard, D. A. and Reddy, J. N.(1989) 'A Model for the Diffusion of Moisture in Adhesive Joints. Part III: Numerical Simulations', The Journal of Adhesion, 27: 1, 41 — 62
To link to this Article: DOI: 10.1080/00218468908050592
URL: http://dx.doi.org/10.1080/00218468908050592

J. Adhesion, 1989, Vol. 27, pp. 41–62
Reprints available directly from the publisher
Photocopying permitted by license only

Printed in the United Kingdom

A Model for the Diffusion of Moisture in Adhesive Joints. Part III: Numerical Simulations

S. ROY

Engg. Sci. & Mechanics Dept., Blacksburg, VA 24061, U.S.A.

D. R. LEFEBVRE

Matls. Engg. Science Dept., Virginia Tech., Blacksburg, VA 24061, U.S.A.

D. A. DILLARD*

Engg. Sci. & Mechanics Dept., Virginia Tech., Blacksburg, VA 24061, U.S.A.

J. N. REDDY

Engg. Sci. & Mechanics Dept., Virginia Tech., Blacksburg, VA 24061, U.S.A.

(Received December 29, 1987; in final form August 12, 1988)

The coupling mechanisms between the diffusion process and the viscoelastic response of an adhesive are explained. A numerical scheme for fully-coupled solutions is proposed and implemented in a two-dimensional finite element code. A number of numerical simulations are presented in order to illustrate the importance of the following features: (1) the bulk viscoelastic behavior, (2) penetrant size, (3) physical aging, (4) the strain dependence of the diffusion coefficient, (5) the concentration dependence of the diffusion coefficient and (6) differential swelling. The effect of moisture intrusion on the stress (strain) distribution across a butt joint is also presented.

KEY WORDS Durability; finite element analysis; viscoelasticity; butt joint; stress; strain.

INTRODUCTION

Governing equations for the diffusion of moisture in adhesive joints were derived in Part I and validated experimentally in Part II. In these preceding sections, the coupling of diffusion kinetics with the mechanical behavior was established. It was shown that the highly nonlinear nature of the governing equations, as well as their implicit time dependence, made the use of an iterative numerical solution necessary.

* To whom correspondence should be addressed.

In Part III, a two-dimensional solution of the fully-coupled diffusion problem is obtained using the finite element code NOVA. NOVA has been under continuous development at Virginia Tech by Reddy and Roy for the past two years. The objective is to provide a more accurate analysis of adhesively-bonded joints.[34–36] In NOVA, the mechanical response of the adhesive layer can be modelled using Schapery's or Knauss' nonlinear single integral constitutive laws for multiaxial states of stress. Penetrant permeation is modelled using the diffusion equations derived in Part I (An extensive validation study of the various original features of the code is presented in References 34 to 36). In this section, one of the most interesting capabilities of NOVA will be demonstrated by a numerical simulation reproducing experimental results featuring a **time-dependent** diffusion coefficient in a poly(styrene) film strained uniaxially. Further, the effect of the various forms of strain coupling on diffusion kinetics will be studied by simulating a butt joint undergoing moisture intake from the edges. The accompanying evolution of the stress and strain fields in the adhesive layer will also be presented.

KNAUSS' NONLINEAR VISCOELASTIC THEORY

Since the diffusion-governing equations are coupled with the mechanical response *via* volumetric strain, constitutive equations for the viscoelastic behavior of the adhesive are also needed in order to solve the fully-coupled diffusion problem. Knauss' nonlinear viscoelasticity theory is the most natural choice for the present study because it employs the same phenomenological description as the diffusion constitutive behavior proposed in Part I. Free volume, in the sense of Turnbull, is used as a unifying parameter to describe changes in the time scale of the viscoelastic response. Specifically, the theory states that mechanical dilatational strain, temperature and sorbent simultaneously act as time-accelerating parameters by dilating the free volume.

In the Knauss approach, the basic single-integral formulation of linear viscoelasticity is used. The stress and strain tensors are related by the Stieltjes convolution integrals and the material is assumed to undergo small deformations.[16] Consider an isotropic polymer. Let $J(t)$ and $B(t)$ be the shear compliance and bulk compliance, respectively. The constitutive equations in the framework of linear viscoelasticity are given by:

$$e_{ij} = \frac{1}{2}\int_{-\infty}^{t} J(t-\xi)\frac{\partial S_{ij}}{\partial \xi}\,d\xi \tag{73}$$

$$\varepsilon_{kk} = \frac{1}{3}\int_{-\infty}^{t} B(t-\xi)\frac{\partial \sigma_{kk}}{\partial \xi}\,d\xi \tag{74}$$

where: e_{ij} = deviatoric strain
ε_{kk} = volumetric strain (mechanical component)
S_{ij} = deviatoric stress
σ_{kk} = volumetric stress

and the indicial summation convention is assumed. The equation numbers are continued from Parts I and II.

Knauss introduced the nonlinearity by expressing that the time scale of viscoelastic response as described by $J(t)$ and $B(t)$ is a strong function of free volume dilatation Δf. The total free volume dilatation Δf is expressed as the sum of a mechanical strain contribution, a thermal expansion contribution and a sorbent expansion contribution:

$$\Delta f = \varepsilon^f_{kk} + \alpha \Delta T + \gamma C \tag{75}$$

where: α = coefficient of thermal expansion of the free volume
γ = coefficient of swelling
ε^f_{kk} = volume dilatation of the free volume due to external loads

The dilatation of the free volume should not be confused with the total volumetric strain appearing in Expression (74). The relationship between these two quantities will be introduced later. Note that expression (75) has been used in our derivation of an expression for the diffusion coefficient in Part I.

Furthermore, Knauss assumed that: (1) free volume changes do not change the distribution function of retardation times in $J(t)$ and $B(t)$, implying that the material is thermorheologically simple, and (2) the same shift factor can be used for both shear and bulk properties. Mathematically, the time is simply shifted by using the differential expression:

$$dt' = \frac{dt}{a(\Delta f)} \tag{76}$$

where t' denotes the reduced time and the shift factor $a(\Delta f)$ is given by:

$$Ln\{a(\Delta f)\} = -\frac{B}{f_0}\frac{\Delta f(T) + \varepsilon^f_{kk} + \gamma C}{f_0 + \Delta f(T) + \varepsilon^f_{kk} + \gamma C} \tag{77}$$

where $\Delta f(T)$ is a function describing thermally-induced changes in the free volume in the temperature domain of interest. For example, $\Delta f(T) = \alpha(T - T_g)$ above T_g.

Thus, Knauss' shift factor is an immediate generalization of the WLF shift factor (expression 20). Note that for $\varepsilon^f_{kk} = 0$ and $\gamma C = 0$, the standard WLF equation is recovered. Knauss' nonlinear constitutive behavior can now be summarized as follows:

$$e_{ij} = \frac{1}{2}\int_{-\infty}^{t} J(\psi - \psi')\frac{\partial S_{ij}}{\partial \tau}\, d\tau \tag{78}$$

$$\varepsilon_{kk} = \frac{1}{3}\int_{-\infty}^{t} B(\psi - \psi')\frac{\partial \sigma_{kk}}{\partial \tau}\, d\tau \tag{79}$$

with:

$$\psi(t) = \int_{-\infty}^{t} \frac{dt'}{a(\Delta f)} \tag{80}$$

$$\psi' = \psi(\tau) = \int_{-\infty}^{\tau} \frac{dt'}{a(\Delta f)} \tag{81}$$

An obvious advantage in using Knauss' constitutive model in our study is that the shift factor subroutine can be shared by both the diffusion code and the viscoelasticity code. Only void size factors B and B^D differ in principle in the two boundary-value problems.

It was noted earlier that NOVA has provision for either the Schapery or Knauss nonlinear viscoelastic theories. The basic form of the constitutive equations is similar in both theories; they only differ by the form and number of nonlinearizing functions. Fortunately, it is possible to reduce Knauss' model as a particular case of Schapery's model by changing the expression for the shift factor and setting the remaining nonlinearizing functions to 1. This scheme was used in the finite element formulation of the viscoelastic behavior in NOVA.

NUMERICAL SCHEME

The coupling between diffusion and viscoelasticity can be easily seen by cross-examining the governing equations for the Diffusion Boundary. Value Problem {DBVP, Expressions (55) to (57)} and the constitutive equations for the Viscoelasticity Boundary-Value Problem {(VBVP, Expressions (78) to (81)}. The diffusion equations are strain dependent, while the viscoelastic behavior is affected by a sorbent concentration term in the shift factor. The mechanical response is also affected by sorbent concentration, in that mechanical strains can be generated due to swelling. This effect is incorporated into the governing equations by stating that the total strain contains a sorbent expansion component.

The interplay between the DBVP and the VBVP is illustrated in Figure 15. Numerically, this coupling can be implemented by solving the diffusion problem

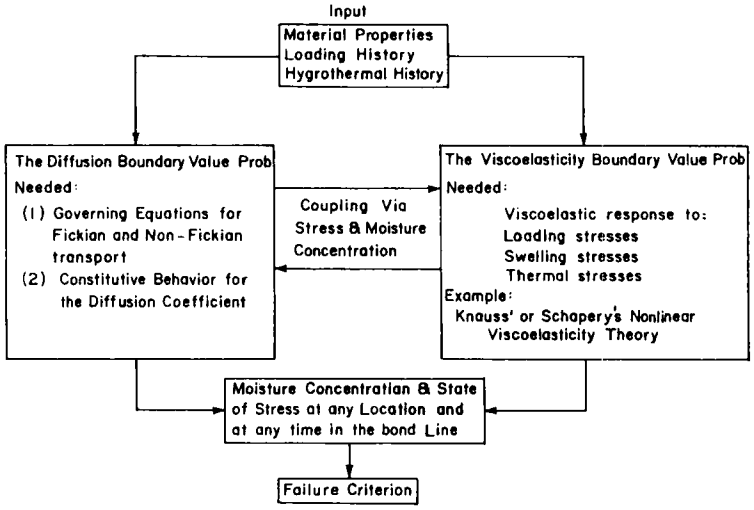

FIGURE 15 Coupling between the DBVP and the VBVP.

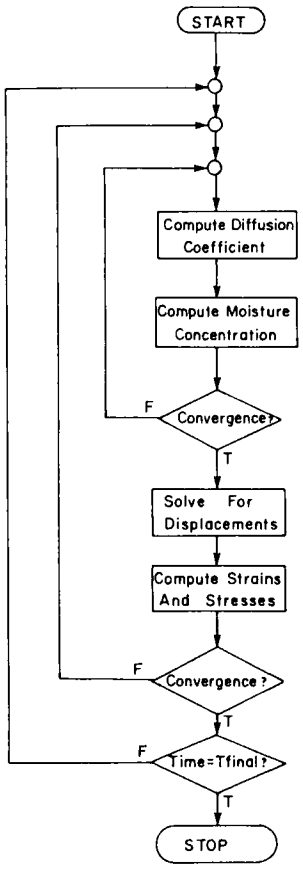

FIGURE 16 Algorithm for the fully coupled problem.

and viscoelasticity problem concurrently in order to update continually the coupling variables, namely, the volumetric strain and sorbent concentration. This scheme has been encoded in NOVA and is summarized by the flow chart shown in Figure 16. Note that the strain dependence of the solubility is not included in this study. The experimental data presented in Part II seem to justify this approximation as long as the penetrant does not show much miscibility with the polymer.

The numerical treatment presented herein introduces an implicit time dependence in the diffusivity and in the solubility, thereby allowing the simulation of more complex sorption behaviors known as "anomalous" or "case II". Case II sorption refers to a case where the rate of transport is entirely governed by the rate of viscoelastic relaxation.[7] Anomalous diffusion refers to an intermediate case between Fickian and Case II diffusion.

FINITE ELEMENT FORMULATION OF THE PROBLEM

Viscoelasticity formulation

The total strain and stress components in a material can be written as the sum of deviatoric and volumetric components:

$$\varepsilon_{ij} = e_{ij} + \tfrac{1}{3}\varepsilon_{kk}\,\delta_{ij} \tag{82}$$

$$\sigma_{ij} = S_{ij} + \tfrac{1}{3}\sigma_{kk}\,\delta_{ij} \tag{83}$$

For a viscoelastic material, the constitutive equations discussed earlier can be rewritten in the following form, if the effects due to loading history prior to $t = 0$ are negligible:

$$\varepsilon_{kk} = \tfrac{1}{3}B(0)\sigma_{kk}(t) + \frac{1}{3}\int_0^t \Delta B(\psi - \psi')\frac{\partial}{\partial\tau}\sigma_{kk}(\tau)\,d\tau \tag{84a}$$

$$e_{ij} = \tfrac{1}{2}J(0)S_{ij}(t) + \frac{1}{2}\int_0^t \Delta J(\psi - \psi')\frac{\partial}{\partial\tau}S_{ij}(\tau)\,d\tau \tag{84b}$$

where ψ and ψ' are given by expressions (80) and (81) respectively.

Using results from Eq. (84) in Eqs. (82) and (83), one obtains for two-dimensional analysis

$$\{\varepsilon\} = [C] * \{d\sigma\} \tag{85a}$$

where:

$$\{\varepsilon\} = \{\varepsilon_{11},\ \varepsilon_{22},\ \gamma_{12},\ \varepsilon_{33}\}^T \tag{85b}$$

$$[C] = \begin{bmatrix} \left(\frac{B}{9}+\frac{J}{3}\right) & \left(\frac{B}{9}+\frac{J}{6}\right) & 0 & \left(\frac{B}{9}-\frac{J}{6}\right) \\ & \left(\frac{B}{9}+\frac{J}{3}\right) & 0 & \left(\frac{B}{9}-\frac{J}{6}\right) \\ & \text{symmetric} & J & 0 \\ & & & \left(\frac{B}{9}+\frac{J}{3}\right) \end{bmatrix} \tag{85c}$$

and:

$$\{d\sigma\} = \{d\sigma_{11},\ d\sigma_{22},\ d\tau_{12},\ d\sigma_{33}\}^T \tag{85d}$$

and where the symbol $(*)$ denotes the convolution operator.

If the transient compliances are now written in the form of a Prony series, then:

$$\Delta B(\psi) = \sum_{r=1}^{n} B_r(1 - \exp(-\psi/\tau_r)) \tag{86a}$$

$$\Delta J(\psi) = \sum_{r=1}^{m} J_r(1 - \exp(-\psi/\eta_r)) \tag{86b}$$

Substituting Eqs. (86a) and (86b) in Eq. (85a) results in a matrix equation given by:

$$\{\varepsilon\} = [N]\{\sigma\} + \{H\} \tag{87}$$

where the matrix $[N]$ contains the instantaneous compliances at time t, and the vector $\{H\}$ contains the components of the hereditary strains. Pre-multiplying Eq. (87) by $[N]^{-1}$ and rearranging,

$$\{\sigma\} = [L](\{\varepsilon\} - \{H\}) \tag{88}$$

where:

$$[L] = [N]^{-1} \tag{89}$$

The finite-element equilibrium equations may be established by invoking the principle of virtual work:

$$\{\delta u\}^T\left(\int_V [B]^T\{\sigma\}\, dV - \{F\}\right) = 0 \tag{90}$$

Using results from Eq. (88) in (90) yields,

$$\{\delta u\}^T\left(\int_V [B]^T[L]\{\varepsilon\}\, dV - \int_V [B]^T[L]\{H\}\, dV - \{F\}\right) = 0 \tag{91}$$

Writing the strain-displacement relations as:

$$\{\varepsilon\} = [B]\{u\} \tag{92}$$

and substituting in (91):

$$\{\delta u\}^T\left(\int_V [B]^T[L][B]\, dV\{u\} - \int_V [B]^T[L]\{H\}\, dV - \{F\}\right) = 0 \tag{93}$$

or simply,

$$\{\delta u\}^T\{R\} = 0 \tag{94}$$

Noting that Eq. (93) contains a source of nonlinearity imbedded in the definition of the shift factor, the Newton–Raphson iteration technique is employed to solve for the displacements.

For the ith iteration, the incremental displacements $\{\Delta u_i\}$ are obtained from:

$$\{\Delta u_i\} = -[K_T]^{-1}\{R_i\} \tag{95}$$

and:

$$\{u_i\} = \{u_{i-1}\} + \{\Delta u_i\} \tag{96}$$

where:

$$[K_T] = \int_V [B]^T[L][B]\, dV \tag{97}$$

Moisture diffusion analysis

The finite element formulation of Fick's Law in two dimensions is developed using the weak variational form;[34–36] the "weak" form of the variational

procedure weakens the continuity requirements on the displacements, by allowing discontinuity in the displacement gradients:

$$\int_{\Omega^e} V \cdot \left[\frac{\partial C}{\partial t} - \frac{\partial}{\partial x}\left(D\frac{\partial C}{\partial x} + KDC\frac{\partial \varepsilon_{kk}}{\partial x}\right) - \frac{\partial}{\partial y}\left(D\frac{\partial C}{\partial y} + KDC\frac{\partial \varepsilon_{kk}}{\partial y}\right)\right] dx\, dy = 0 \tag{98}$$

For the plane strain case, the volumetric strains can be expressed as

$$\varepsilon_{kk} = \frac{\partial u}{\partial x} + \frac{\partial v}{\partial y} - \gamma C - \alpha\, \Delta T \tag{99}$$

Assuming that the moisture concentration may be approximated by:

$$C(x, y, t) = \sum_{j=1}^{n} \psi_j(x, y) C_j(t), \tag{100}$$

and the test function in expression (98) may be set to be equal to the interpolation function:

$$V = \psi_i \tag{101}$$

Substitution of Eq. (100) into the weak form of Eq. (98) (see Reddy[34]) gives

$$[M^e]\{\dot{C}\} + [K^e]\{C\} = \{F^e\} \tag{102}$$

where:

$$[M^e] = \int_{\Omega^e} \psi_i \psi_j\, dx\, dy \tag{103}$$

$$[K^e] = \int_{\Omega^e} D\left(\frac{\partial \psi_i}{\partial x}\cdot\frac{\partial \psi_j}{\partial x} + \frac{\partial \psi_i}{\partial y}\cdot\frac{\partial \psi_j}{\partial y}\right) dx\, dy \tag{104}$$

$$\{F^e\} = -\int_{\Gamma^e} \psi_i \hat{q}\, dS - K\int_{\Omega^e} \left\{D\cdot\left(\sum_{j=1}^{n} \psi_j C_j\right)\left[\left(\frac{\partial^2 u}{\partial x^2} + \frac{\partial^2 v}{\partial x\, \partial y} - \gamma\frac{\partial C}{\partial x} - \alpha\frac{\partial \Delta T}{\partial x}\right)\frac{\partial \psi_i}{\partial x} + \left(\frac{\partial^2 u}{\partial x\, \partial y} + \frac{\partial^2 v}{\partial y^2} - \gamma\frac{\partial C}{\partial y} - \alpha\frac{\partial \Delta T}{\partial y}\right)\frac{\partial \psi_i}{\partial y}\right]\right\} dx\, dy \tag{105}$$

and:

$$\hat{q} = -D\left\{\left(\frac{\partial C}{\partial X} + KC\frac{\partial \varepsilon_{kk}}{\partial x}\right)n_x + \left(\frac{\partial C}{\partial y} + KC\frac{\partial \varepsilon_{kk}}{\partial y}\right)n_y\right\} \tag{106}$$

The time derivative $\{\dot{C}\}$ is approximated by using the θ-family of approximation for the nth time step,

$$\theta\{\dot{C}\}_{n+1} + (1-\theta)\{\dot{C}_n\} = (\{C\}_{n+1} - \{C\}_n)/\Delta t_{n+1} \quad \text{for} \quad 0 \le \theta \le 1 \tag{107}$$

where θ is a weighting parameter. From equations (99) and (106), we obtain for each element,

$$[A^e]\{C\}_{n+1} - [B^e]\{C\}_n - \{P^e\}_n = \{0\} \tag{108}$$

where:

$$[A^e] = [M^e] + \theta \Delta t_{n+1}[K^e] \tag{109}$$

$$[B^e] = [M^e] - (1 - \theta)\Delta t_{n+1}[K^e] \tag{110}$$

$$[P^e] = \Delta t_{n+1}(\theta\{F^e\}_{n+1} + (1 - \theta)\{F^e\}_n) \tag{111}$$

Recognizing that a source of nonlinearity in the form of the diffusion coefficient D is imbedded in the matrix $[K^e]$, the Newton–Raphson technique is employed to solve for the moisture concentrations $\{C\}_{n+1}$ at each time step.

VALIDATION PROBLEM: VISCOELASTIC DIFFUSION THROUGH A POLY(STYRENE) FILM

Smith *et al.*[37,38] conducted a permeation experiment to study gas transport in polystyrene and found that the diffusion coefficient for CO_2, Ar and Xe decreased with time when the polystyrene film was subjected to a constant uniaxial strain. Figures 17 and 18 reproduce experimental results from Reference 37. Figure 17 illustrates the time dependence of the diffusion coefficient for CO_2 in a Trycite film (biaxially oriented poly(styrene) film) at different strains at 50 °C. The reference diffusion coefficient D_0 was taken prior to stretching. Figure 18 illustrates the time dependence of the diffusion coefficient for CO_2 and Xe in a Trycite film at the same strain level at 50 °C. In this case, the reference diffusion coefficient D_1 was measured one hour after stretching.

The reason these experimental data were found to be convenient for a test of NOVA is that poly(styrene) is adequately characterized mechanically. Reference

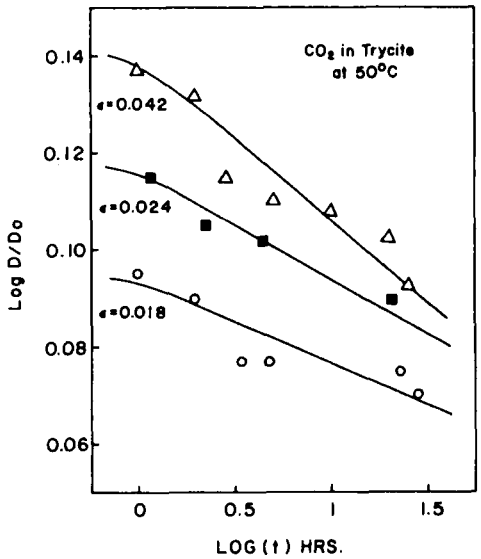

FIGURE 17 Time dependence of D; carbon dioxide diffusion through a trycite film at 50°C subjected to different strain levels. D_0 was taken before stretching.[37]

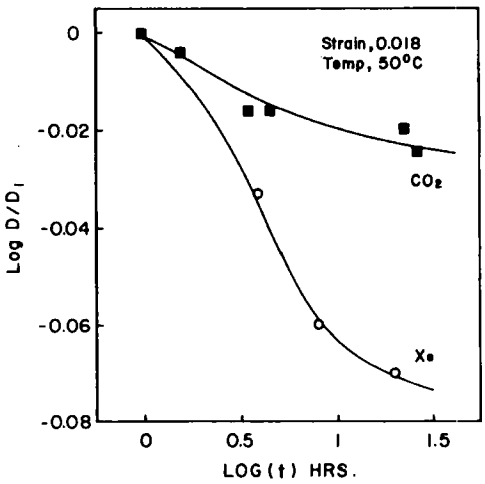

FIGURE 18 Effect of penetrant size on D; trycite film at 50°C, subjected to a strain of 0.018. D_1 was taken one hour after stretching.[37]

13 gives the viscoelastic shear compliance and the viscoelastic bulk compliance of poly(styrene) around the glass transition temperature (100°C). Bulk properties are rarely documented in the literature, mainly due to a lack of recognition of their importance, compounded by complexities in the measurement techniques. Since our study establishes that the diffusion behavior as well as the nonlinear viscoelastic behavior are controlled by volumetric properties, we conclude that adequate bulk viscoelastic characterization will be an absolute necessity for improved diffusion predictions.

Although the shear compliance and bulk compliance are given for two different molecular weights (500,000 and 600,000 respectively), the properties were assumed to be usable for any high molecular weight poly(styrene). This assumption is valid as long as the molecular weight is large compared to some critical value {38,000 for poly(styrene)} corresponding to the onset of entanglement coupling.[13]

The compliances around 100°C given in Reference 13 were curve-fitted with a Prony Series using a nonlinear least-square fitting routine. Since predictions must be compared to data at 50°C, a time-temperature shift had to be performed. It is well known that the shift factor below the glass transition temperature is governed by an activation energy instead of an activation volume, as in the case of the rubbery state. The shift factor is given by:

$$a = \exp\left[\frac{\Delta H}{R}\left(\frac{1}{T_R} - \frac{1}{T}\right)\right] \tag{112}$$

where: ΔH = activation energy
R = the gas constant
T_R = reference temperature
T = temperature

Values of ΔH between 30 kcal/mole and 40 kcal/mole have been suggested by Ferry[13] and Matsuoka.[17] A value of 35 kcal/mole was taken in our study, which corresponds to a shift factor of 1500. This means that the retardation times at 50°C are 1500 times larger than at 100°C, reflecting the slower mechanical response of the material at a lower temperature (time in sec). The same shift factor was used for the bulk compliance and the shear compliance.[17]

The reference temperature T_0 for the diffusion problem was fixed at 50°C and the reference diffusion coefficient D_0 was taken from the measured values at 50°C in Reference 37. Since all the data points in Reference 37 are given at 50°C, the temperature term in the shift factor was set to zero in all the computations. The swelling coefficient of expansion γ was set to zero because the sorbents used in the permeation studies have little chemical affinity with poly(styrene).

At this point, it is useful to recall that the volumetric strain ε^f_{kk} contained in the diffusion equation corresponds to the dilatation of the free volume and not to the mechanical volumetric strain ε_{kk}, used in the governing equations for viscoelasticity. Kovac's model presented in Reference 13 postulates that the free volume dilatational strain ε^f_{kk} is equal to the transient component of the mechanical strain ε_{kk}. Kovac's approach was used, and the free volume dilatation strain at any time was given by:

$$\varepsilon^f_{kk} = \varepsilon_{kk} - 3B_0\sigma_{kk} \tag{113}$$

At infinite times, one finds that ε^f_{kk} is approximately equal to one half of ε_{kk}, which is consistent with remarks made previously in Part II.

Figures 19, 20 and 21 show numerical simulations produced by NOVA, of the problem studied by Smith *et al* in Reference 37. Figure 19 shows the variation of the diffusion coefficient with time for the three strain levels indicated in Figure 17.

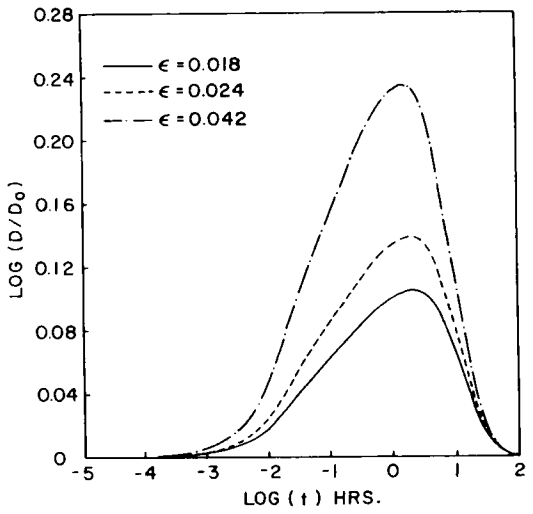

FIGURE 19 Time dependence of D in a polystyrene film at 50°C and influence of the strain level; numerical simulation with $B^D = 0.25$. D_0 was taken before stretching.

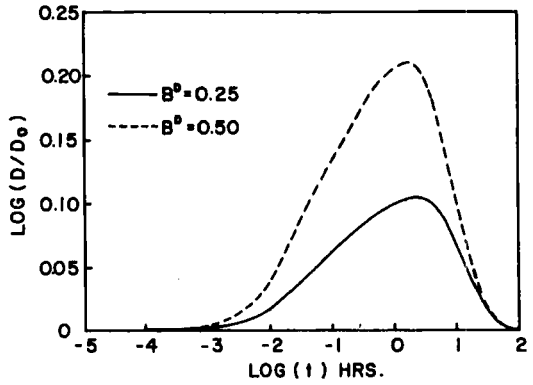

FIGURE 20 Time dependence of D in a polystyrene film at 50°C and influence of the void size parameter; numerical simulation with $\varepsilon = 0.018$. D_0 was taken before stretching.

From Figure 19, it is evident that, independently of the strain level, the diffusion coefficient reaches a peak at $t = 1$ hour and then slowly decays back to the reference value D_0. This behavior can be attributed to an initial increase in the free volume due to the application of the uniaxial strain, followed by a continuous recovery in free volume at constant strain, as the poly(styrene) film undergoes shear relaxation which gradually reduces the hydrostatic stress level. A larger applied strain produces larger initial dilatation, resulting in a higher peak in the diffusion coefficient. Figure 19 also reveals that the rate of change of the diffusion coefficient (to be paralleled with the rate of change of the free volume) becomes larger as the applied strain level increases. This strain level dependence in the response rate is an excellent illustration of the nonlinear nature of the mechanical response, described here by Knauss' model. It should be noted that the initial

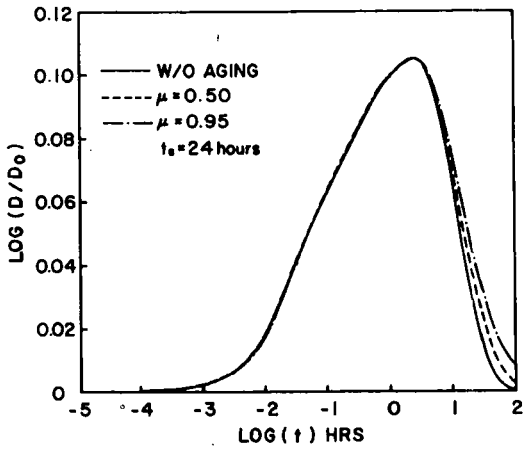

FIGURE 21 Time dependence of D in a polystyrene film at 50°C and influence of physical aging; numerical simulation with $B^D = 0.25$ and $\varepsilon = 0.018$.

increase in the diffusion coefficient is largely due to the fact that bulk creep occurs on a much shorter time scale than creep in shear. (Our data indicate a shift of about five decades between the bulk retardation spectrum and the shear retardation spectrum). It is instructive to compare our numerical simulation in Figure 19 with the experimental data shown in Figure 17. Upon examining the time scale of Figure 19, it becomes clear that the initial increase in the diffusion coefficient was not experimentally accessible to Smith *et al.* For this reason, the initial transient response was seen as instantaneous by Smith *et al.* and only the relaxation part of the curve is shown in Figure 17. When Figures 17 and 19 are compared, it becomes apparent that the right hand side of Figure 19 correlates very nicely, although not exactly with the experimental results in Figure 17.

The influence of penetrant molecule size on the diffusion coefficient for gases in poly(styrene) was qualitatively studied by varying the magnitude of the void size parameter B^D. Levita and Smith[37] explained that, due to molecular shape effects, the effective critical void size of a CO_2 molecule is larger than that of xenon. It follows, from our discussion in Part I, that B^D for CO_2 should be smaller than that of xenon (B^D and the critical void size V_C are inversely related). Figure 20 shows predictions obtained from NOVA for two values of B^D and a strain of 1.8% in a poly(styrene) film. Before comparing predictions with experiment, it is important to note that the reference states used are not the same: In Figure 20 the reference diffusion coefficient (D_0) was taken before stretching whereas, in Figure 18, Levita and Smith used the diffusion coefficient measured one hour after stretching (D_1). With this information in mind, it can be seen by comparing Figures 18 and 20 that NOVA correctly predicts that a smaller penetrant molecular size leads to a faster rate of decrease in the diffusion coefficient. Since the actual B^D values for CO_2 and Xe are unknown, the above comparison is only qualitative at this point.

The effect of physical aging on the diffusion coefficient was studied by implementing equation (31) of Part I in NOVA. The penetrant was CO_2 and the values of temperature strain and t_e were set at 50°C, 1.8% and 24 hours, respectively. Figure 21 shows that a faster rate of physical aging, denoted by a higher value of parameter μ, causes the diffusion coefficient to decay more slowly. This behavior is expected, since a smaller free volume causes molecular relaxation processes to occur over a larger period of time. Unfortunately, no experimental data are available for comparison here.

DIFFUSION KINETICS IN A BUTT JOINT

In this section, a number of numerical simulations of moisture diffusion in the adhesive layer of a butt joint are presented. The main emphasis is on evaluating the relative importance of the various coupling effects between diffusion and mechanical strain (stress). In order to achieve this goal, a parametric study was carried out using realistic values for the adhesive properties. The adhesive mechanical properties were those of poly(styrene) at 50°C. (Since we are

TABLE III
Summary of butt joint simulations

Case #	Strain dependence in D & a	Concentration dependence in D & a	Strain-induced driving force	Mechanical BCs (longitudinal strain)
1	No	No	No	2%
2	Yes	No	No	2%
3	Yes	Yes*	No	2%
4	Yes	Yes*	Yes	2%

(*$\gamma = 0.01$).

concerned primarily with the rate of bulk diffusion, the fact that poly(styrene) does not adhere well to metal surfaces will have no bearing on our general conclusions on durability). In order to study the effect of swelling, a large value for the coefficient of swelling expansion (γ) was needed. Since γ for poly(styrene) is negligible, a fictitious material combining the mechanical properties of poly(styrene) and the coefficient of swelling expansion of a moderately hydrophilic polymer ($\gamma = 0.01$) was used.

Table III summarizes the four cases investigated in the parametric study. (The numbering of the cases run should not be confused with the fundamental modes of sorption known as "Case I" and "Case II"). The joint geometry and finite element discretization are given in Figure 22. Note that the mechanical boundary conditions used were a uniform axial displacement resulting in a uniform strain of 2% in the adhesive layer. The normalized moisture concentration at the free edge of the adhesive layer is unity and the initial concentration throughout the adhesive layer is zero.

Figure 23 shows the moisture concentration profiles within the adhesive layer at three different times when there is no coupling (Case 1). In this case, the diffusion coefficient remains constant with time, that is, $D = D_0$. Case 1 is the classical Fickian diffusion in a plane sheet for which a closed-form solution is available.

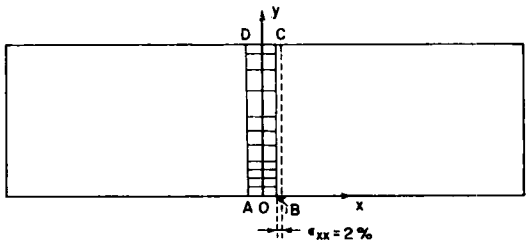

DIFFUSION BOUNDARY CONDITIONS:
AB : $\bar{C} = 1$
DC : $\bar{C} = 0$
BC : $J = 0$
AD : $J = 0$

FIGURE 22 Butt joint geometry and bond line discretization; total length = 200.5, width = 30.0 and bond thickness = 0.25.

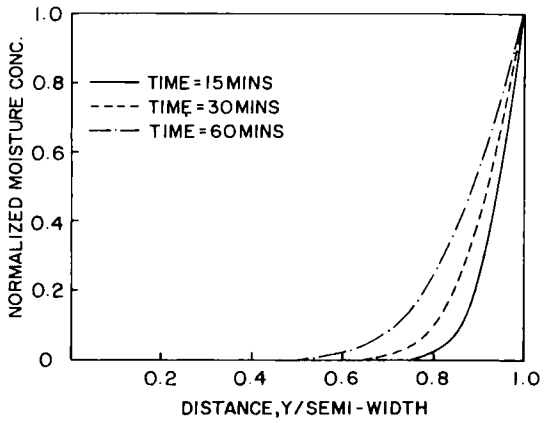

FIGURE 23 Simulation of diffusion in a butt joint (Case 1); moisture profiles within the adhesive in the absence of coupling.

For short times, as in our simulations, the sheet may be considered as a semi-infinite medium and the following approximation is convenient:

$$\bar{C}(t, y) = \text{erfc}(y/2\sqrt{D_0\, t}) \tag{114}$$

where erfc is the error function complement.

Figure 24 shows the moisture concentration profiles for the case where there is viscoelastic coupling only, that is, when both the diffusion coefficient and the shift factor are dependent on the transient component of the dilatational strain (Case 2).

Figure 25 depicts the case where there is full coupling in the diffusion coefficient and in the shift factor. This means that the diffusion coefficient and the shift factor are both a function of the dilatational strain and of the moisture

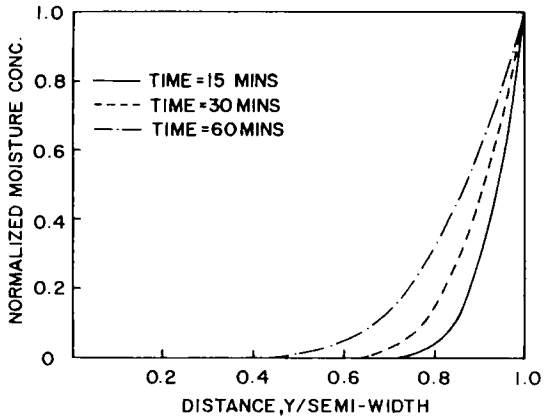

FIGURE 24 Simulation of diffusion in a butt joint (Case 2); moisture profiles within the adhesive with a strain dependence in D.

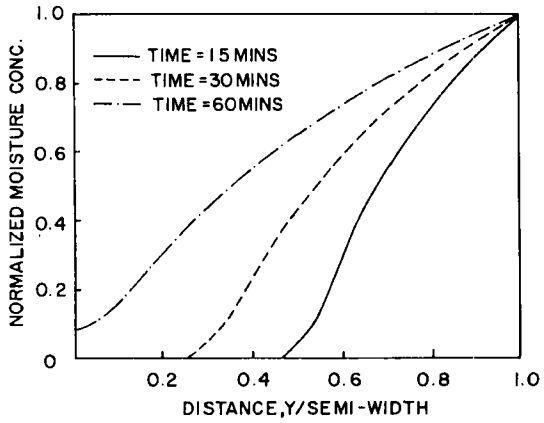

FIGURE 25 Simulation of diffusion in a butt joint (Case 3); moisture profiles within the adhesive with a strain and concentration dependence in D.

concentration at any given point in the adhesive. Note the dramatic increase in penetration rate relative to the two previous cases, as well as the convex shape of the concentration profiles. The moisture profiles for the fully-coupled diffusion problem (Case 4) are not shown because they are indistinguishable from those plotted in Figure 25 (Case 3). In addition to all the features of Case 3, Case 4 includes the contribution of the strain-induced driving force ∇W_p. This last case required the use of 135 time steps, compared to about 50 time steps for Case 1.

Lastly, Figure 26 presents the results for each of the four previous cases, for comparison at time $t = 60$ minutes. Note that Case 3 and Case 4 are still indistinguishable after 60 minutes. Only strain and concentration coupling in the diffusion coefficient seem to have a significant accelerating effect. Of course, the effect of differential swelling would have appeared if a larger value of the

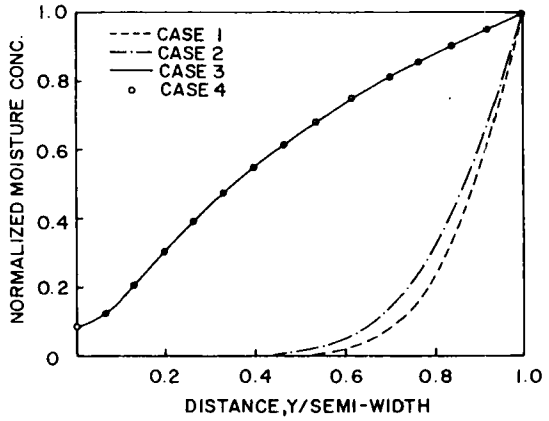

FIGURE 26 Comparison between Cases 1, 2, 3 and 4; moisture profile within the adhesive at $t = 60$ min.

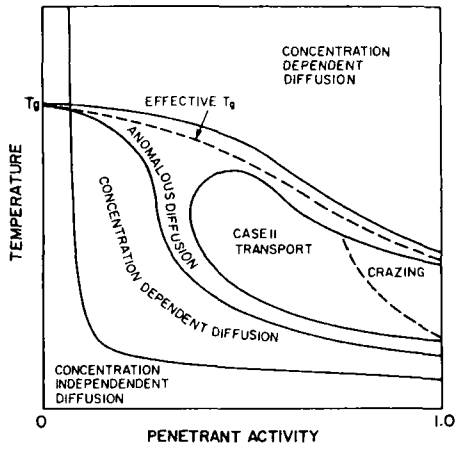

FIGURE 27 Hopfenberg–Frisch chart of anomalous diffusion; effect of penetrant activity on transport kinetics.[26]

coefficient of moisture expansion had been used. High magnitudes for γ, promoting Case II kinetics, are encountered when the penetrant is a good solvent of the polymer. For structural adhesives in the presence of moisture, however, γ is expected to be close to 0.01. (An estimate of γ from data in Reference 39 yields a value of 0.014 for a 3501-6 epoxy). The various types of diffusion behaviors in polymers have been graphically summarized by Hopfenberg and Frish[6] in terms of penetrant activity and temperature (see Figure 27). Examination of this chart confirms that non-Fickian driving forces are not operative below T_g as long as penetrant activity is small, and that a concentration-dependent diffusion coefficient is then sufficient to describe the transport behavior.

The main findings from this study may be summarized as follows:

1. The mechanical and hygroelastic coupling terms in the diffusion coefficient must be included in a durability analysis, due to their substantial accelerating effect on penetration kinetics.
2. The effect of differential swelling can be counted as negligible for a typical structural adhesive. Polymers for which this extra driving force becomes important are not likely to be selected for adhesive applications, due to their poor performance in moist environments.

EVALUATION OF THE STRESS AND STRAIN FIELDS IN A BUTT JOINT UPON MOISTURE PENETRATION

The results presented in this section were generated by running Case 3 (see Table III) with NOVA. The bond line discretization, mechanical boundary conditions and material properties were the same as earlier (same γ and same mechanical

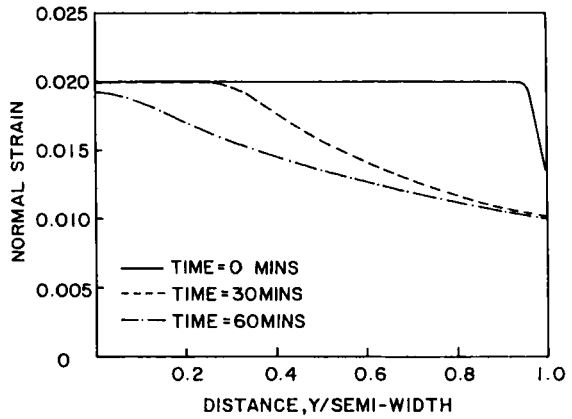

FIGURE 28 Simulation of the strain distribution in a butt joint (Case 3); variation of the normal strain distribution in the adhesive accompanying moisture diffusion.

properties). The stress and strain distributions were plotted at three different elapsed times: 0 min., 30 min. and 60 min. On each of these plots, the free edge OB of the butt joint is located at the right-hand side and the distance along the bond line is normalized with respect to the semi-width of the joint.

Figures 28 and 29 illustrate the effect of moisture-induced swelling on the mechanical component of normal strain ε_{xx} transverse strain ε_{yy}, respectively. In Figure 28, the absorbed moisture induces swelling strains within the adhesive, resulting in a lower value of ε_{xx}. Note that ε_{xx} refers to the **mechanical** component of strain. In the boundary-value problem considered here, three types of strains are used: the mechanical strain, the hygroscopic strain and the kinematic strain. The kinematic strain (2% here) always remains equal to the sum of the mechanical and hygroscopic strains. Since the boundary conditions used

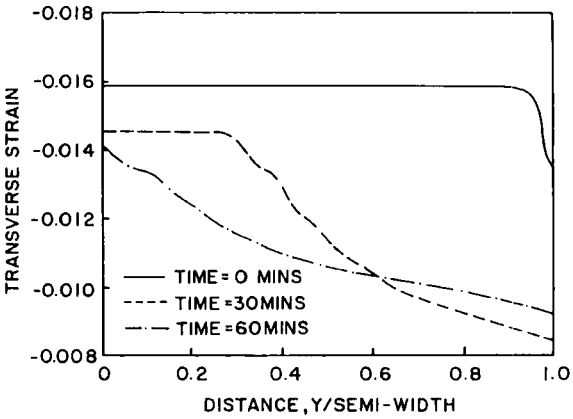

FIGURE 29 Simulation of the strain distribution in a butt joint (Case 3); variation of the transverse strain distribution in the adhesive accompanying moisture diffusion.

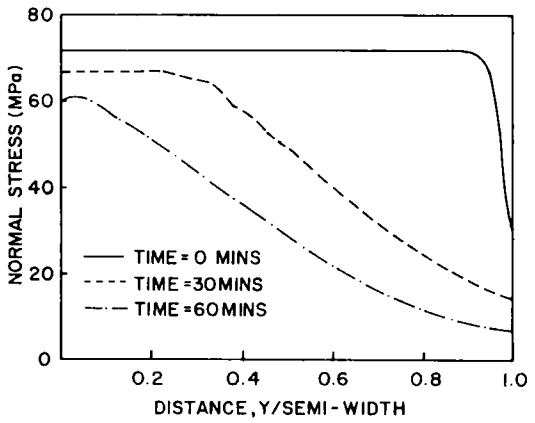

FIGURE 30 Simulation of the stress distribution in a butt joint (Case 3), variation of the normal stress distribution in the adhesive accompanying moisture diffusion.

impose a uniform, positive, kinematic normal strain of two percent initially, the lower values of mechanical strain ε_{xx} in the presence of moisture-remain positive. Note that in an unloaded butt joint, ε_{xx} would have become negative, reflecting the constraining effect of the stiff adherends surrounding the adhesive. By comparing Figure 28 with Figure 25, it appears quite clear that the region with a lowered normal strain corresponds to the domain occupied by moisture.

Figure 29 shows a negative initial transverse strain resulting from the transverse Poisson's contraction upon loading. In the absence of moisture, the algebraic value of ε_{yy} would tend to increase initially and then decrease, due to the transient bulk response of the polymer. The initial bulk creep can be seen here in the unperturbed region at time = 30 min., causing the Poisson's ratio to decrease. The subsequent bulk relaxation can be seen near the free edge as the Poisson's ratio increases again at longer times. As in the case of the normal strain, moisture-induced swelling causes an abrupt change in the distribution of ε_{yy}, and the transverse strain distribution in the dry region seems to be unchanged.

Figure 30 depicts the effect of moisture-induced swelling on the distribution of normal stress σ_{xx}. The comments made for ε_{xx} in Figure 28 can be repeated here. The only difference in behavior is found in the dry region ahead of the moisture front, where a stress reduction due to viscoelastic relaxation can be seen.

CONCLUSIONS

Governing equations for the diffusion of small molecules in polymers have been derived and incorporated into a two-dimensional finite element code. In the case of an adhesive joint, simulations have shown that the main accelerating effects in the diffusion rate of moisture through the bond line can be traced to the strain

and concentration dependence of the diffusion coefficient, the latter playing a predominant role.

Invariably, the development of powerful predictive capabilities raises the question of the adequacy of material characterization. A main finding of this study is that the bulk properties (also called volumetric properties) of the adhesive play a central role in the coupling mechanisms between the diffusion behavior and the viscoelastic response. Unfortunately, the bulk characterization of polymers has not received proper attention in experimental mechanics. This trend must be reversed if rigorous predictions of the hygromechanical behavior of adhesives are sought.

NOTATION

ε_{ij}: Strain components produced due to applied mechanical stress.
e_{ij}: Deviatoric strain components.
ε_{kk}: Dilatational strain
ε^f_{kk}: Transient component of mechanical strain ε_{kk}
σ_{ij}: Cauchy stress tensor
S_{ij}: Deviatoric stress components
σ_{kk}: Dilatational stress
$B(0)$: Bulk compliance at time $t = 0$
$\Delta B(\psi)$: Transient bulk compliance
$J(0)$: Shear compliance at time $t = 0$
$\Delta J(\psi)$: Transient shear compliance
ψ: Reduced time
$a(\Delta f)$: Shift factor
M_r: Constant coefficient in Prony series
J_r: Constant coefficient in Prony series
τ_r: Retardation time for bulk compliance
η_r: Retardation time for shear compliance
δ_{ij}: Kronecker delta
$\{\delta u\}$: First variation in displacement
$[B]$: Strain displacement transformation matrix
$\{F\}$: Vector of external forces
$[K_T]$: Tangent stiffness matrix
Ω^e: Domain of integration (area)
Γ^e: Path of integration (Line)
V: Test function
$C(x, y, t)$: Moisture concentration
D: Diffusion coefficient
K: A material constant
$\psi_j(x, y)$: Interpolation function for jth node
$C_j(t)$: Moisture concentration at jth node
γ: Coefficient of expansion due to moisture sorption

α: Coefficient of thermal expansion
ΔT: Temperature change
Δt_{n+1}: Step-size for the nth time step
n_x: x-direction cosine for unit vector normal to the boundary
n_y: y-direction cosine for unit vector normal to the boundary

References

1. Y. Weitsman, *J. Mech. Phys. Solids* **35,** 73 (1987).
2. M. Tirrell and M. F. Malone, *J. Polym. Sci. Polym. Physics Ed.* **15,** 1569 (1977).
3. J. Crank, *The Mathematics of Diffusion, 1st. Ed.* (Oxford at the Clarendon Press, London, 1956).
4. H. L. Frisch, T. T. Wang and T. K. Kwei, *J. Polym. Sci.* **A-2,** 879 (1969).
5. N. L. Thomas and A. H. Windle, *Polymer* **23,** 529 (1982).
6. R. M. Felder and G. S. Huvard, *Methods of Experimental Physics,* Vol. 16, R. A. Fava, Ed. (Academic Press, New York, 1980), Chap 17, pp. 315–377.
7. J. Comyn, *Polymer Permeability* (Elsevier Applied Science Publishers, London and New York, 1985), Chap. 2–3, pp. 11–117.
8. F. A. Long and D. Richmond, *J. American Chem. Soc.* **82,** 513 (1960).
9. P. Neogi, M. Kim and Y. Yang, *AICHE Journal* **32,** 1146 (1986).
10. D. Turnbull and M. H. Cohen, *J. Chem. Phys.* **34,** 120 (1961).
11. M. H. Cohen and D. Turnbull, *ibid.* **31,** 1164 (1953).
12. P. B. Macedo and T. A. Litovitz, *ibid.* **48,** 845 (1965).
13. J. D. Ferry, *Viscoelastic Properties of Polymers,* 3rd. Ed. (John Wiley and Sons Inc., New York, 1980).
14. J. S. Vrentas, J. L. Duda, H. C. Ling and A. C. Jau, *J. Polym. Sci., Polym. Phys. Ed.* **23,** 289 (1985).
15. J. H. Noggle, *Physical Chemistry* (Little, Brown and Company, Boston, 1985), Chap. 9, pp 445–449.
16. W. G. Knauss and J. J. Emri, *Composites and Structures* **13,** 123 (1981).
17. S. Matsuoka, G. H. Frederickson and G. E. Johnson, *Lecture Notes in Physics 277, Molecular Dynamics and Relaxation Phenomena in Glasses,* T. Dorfmuller and G. Williams, Eds. (Springer-Verlag, Berlin, 1985), p. 188–202.
18. L. C. E. Struik, *Physical Aging in Amorphous Polymers and Other Materials* (Elsevier, Amsterdam, 1978), Chap. 10, pp. 125–134.
19. M. J. Adamson, *Some Free Volume Concepts of the Effects of Absorbed Moisture on Graphite/Epoxy Composite Laminates,* in Adhesion Science Review, Vol. 1, H. F. Brinson, J. P. Wightman and T. C. Ward, Eds. (Commonwealth Press, Inc., Richmond, Virginia, 1987), pp. 87–101.
20. A. Cochardt, G. Shoeck and H. Wiedersich, *Acta Metallogr.* **3,** 533 (1955).
21. F. S. Ham, *J. Appl. Phys.* **30,** 915 (1959).
22. G. Akay, *Polym. Engg. and Sci.,* **22,** 798 (1982).
23. P. J. Flory, *Principles of Polymer Chemistry* (Cornell University Press, Ithaca, 1983), pp. 495–440.
24. A. Peterlin, *J. Macromol. Sci. Physics,* **B11,** 57 (1975).
25. H. Yasuda and A. Peterlin, *J. Appl. Polym. Sci.* **18,** 531 (1976).
26. J. C. Phillips and A. Peterlin, *Polym. Engg. and Sci.* **23,** 734 (1983).
27. J. S. Vrentas, J. L. Duda and Y. C. Ni, *J. Polym. Sci., Polym. Phys. Ed.* **15,** 2039 (1977).
28. R. W. Seymour and S. Weinhold, *Proceedings of Ryder Conference '85, Ninth International Conference on Oriented Plastic Containers,* p. 281 (1985).
29. L. H. Wang and R. S. Porter, *J. Polym. Sci., Polym. Phys. Ed.* **22,** 1645 (1984).
30. P. Zoller and P. Balli, *J. Macromol. Sci. Physics* **B18,** 555 (1980).
31. *Ultem Polyetherimide 1987 Property Guide,* GE Plastics, Ultem Products Operation, Pittsfield, MA, U.S.A.
32. S. Putter and S. Shimabukuro, *SM Report 87–10,* Grad. Aer. Labs., Cal Tech, Pasadena, CA, U.S.A., April 1987.
33. R. Brandes, *personal communication,* GE Plastics Division, Pittsfield, MA, U.S.A.

34. J. N. Reddy and S. Roy, *Report No. VPI-E-85.18,* Department of Engineering Science and Mechanics, VPI & SU, Blacksburg, VA, U.S.A. (1985).
35. S. Roy and J. N. Reddy, *Report No. VPI-E-86.28,* Department of Engineering Science and Mechanics, VPI & SU, Blacksburg, VA, U.S.A. (1986).
36. S. Roy, *PhD Dissertation,* VPI & SU, Blacksburg, VA, U.S.A. (1987).
37. G. Levita and T. L. Smith, *Polym. Engng. and Sci.* **21,** 936 (1981).
38. T. L. Smith, W. Opperman, A. H. Chan and G. Lenta, *Polymer Preprints* **24(1),** 83 (1983).
39. G. S. Springer, *Environmental Effects on Composite Materials, Vol. 2* (Technomic Publishing Company, Inc., 1984), pp. 15, 302.